



ELSEVIER

Journal of Power Sources 97–98 (2001) 332–335

JOURNAL OF  
**POWER  
SOURCES**

www.elsevier.com/locate/jpowsour

# Low temperature lithium manganese cobalt oxide spinels, $\text{Li}_{4-x}\text{Mn}_{5-2x}\text{Co}_{3x}\text{O}_{12}$ ( $0 \leq x \leq 1$ ), for use as cathode materials in rechargeable lithium batteries

A.D. Robertson, A.R. Armstrong, P.G. Bruce\*

School of Chemistry, University of St. Andrews, St. Andrews, Fife KY16 9ST, Scotland, UK

Received 20 June 2000; accepted 30 December 2000

## Abstract

Low temperature synthesis of the lithium-rich cubic spinel  $\text{Li}_4\text{Mn}_5\text{O}_{12}$  with an oxidation state very close to +4 is described. The effect of doping this compound with cobalt according to the solid solution mechanism  $\text{Li}_{4-x}\text{Mn}_{5-2x}\text{Co}_{3x}\text{O}_{12}$  up to the solid solution limit,  $\text{LiMnCoO}_4$ , has also been explored. The evolution of the structure and electrochemistry with increasing cobalt doping is described. With increasing  $x$  there is increasing population of the tetrahedral 8a site by transition metal ions reaching 25% occupancy by Co at  $\text{LiMnCoO}_4$  with corresponding displacement of Li to 16d sites. The optimum performance was obtained for the composition  $\text{Li}_{3.75}\text{Mn}_{4.5}\text{Co}_{0.75}\text{O}_{12}$  which yields a capacity of 150 mA g<sup>-1</sup> at a rate of 25 mA g<sup>-1</sup> (equivalent to C/6) with no perceptible capacity loss, in sharp contrast to the pure Mn materials. © 2001 Elsevier Science B.V. All rights reserved.

**Keywords:** Lithium batteries; Lithium-rich cubic spinel; Lithium intercalation

## 1. Introduction

In the search for lithium intercalation compounds that are suitable for use as positive electrodes in rechargeable lithium batteries, lithium manganese oxides have received a great deal of attention. Such attention has been based on their potential to deliver low cost, lower toxicity and safer materials than  $\text{LiCoO}_2$  or its derivatives. Unfortunately, stoichiometric lithium manganese oxides can suffer from poor stability on cycling, however radical improvements may be obtained by doping. Many dopants have been investigated but Co has proved to be particularly effective. Interest in compounds based on layered  $\text{LiMnO}_2$  has grown substantially in the last two years. We have shown that by doping layered  $\text{LiMnO}_2$  with just 2.5% Co the capacity may be raised from around 140 to 200 mAh g<sup>-1</sup> with a fade of only 0.08% per cycle even at relatively high rates [1].

Within the Li–Mn–O system, compounds with the spinel structure have received special attention in the context of positive electrodes for rechargeable lithium batteries [2–6]. In part this arises from the structure's tolerance towards

doping. A wide variety of dopant ions have been introduced including Li, Co, Ni, Cr, Al, Ga and B [3,6–12]. Attention has focused largely on spinels based on high temperature  $\text{LiMn}_2\text{O}_4$  despite the fact that low temperature spinels such as  $\text{Li}_2\text{Mn}_4\text{O}_9$  and  $\text{Li}_4\text{Mn}_5\text{O}_{12}$  have been known for a number of years [13,14]. Formally, these low temperature spinels may be derived from  $\text{LiMn}_2\text{O}_4$  by introducing, respectively, vacancies or additional lithium into the  $\text{LiMn}_2\text{O}_4$  structure. For example, in the case of the lithium-rich compounds a solid solution series,  $\text{Li}_{1+x}\text{Mn}_{2-x}\text{O}_4$  exists, where  $0 \leq x \leq 1/3$ . The formula for the lithium-rich end-member of this series may be written as  $\text{Li}[\text{Li}_{1/3}\text{Mn}_{5/3}]\text{O}_4$  but is more commonly known as  $\text{Li}_4\text{Mn}_5\text{O}_{12}$ . Like  $\text{LiMn}_2\text{O}_4$ ,  $\text{Li}_4\text{Mn}_5\text{O}_{12}$  is also a cubic spinel. Whereas the overall Mn oxidation state in  $\text{LiMn}_2\text{O}_4$  is +3.5, in the case of  $\text{Li}_4\text{Mn}_5\text{O}_{12}$  manganese is in the +4 oxidation state. These highly oxidised compounds are generally referred to as low temperature spinels because, if synthesised in air, temperatures of around 400°C must be used in order to promote the high Mn oxidation state. These materials are known to act as intercalation hosts for lithium. The doping of low temperature spinels has received much less attention than the high temperature spinel materials [15].

In this paper, we describe the synthesis of  $\text{Li}_4\text{Mn}_5\text{O}_{12}$  with an oxidation state very close to +4. We also explore doping this lithium-rich low temperature spinel with cobalt

\* Corresponding author. Tel.: +44-1334-463800;  
fax: +44-1334-463808.  
E-mail address: p.g.bruce@st-and.ac.uk (P.G. Bruce).

according to the solid solution mechanism  $\text{Li}_{4-x}\text{Mn}_{5-2x}\text{Co}_{3x}\text{O}_{12}$  up to the solid solution limit  $\text{LiMnCoO}_4$ . The evolution of the structure and electrochemistry with Co doping is described. The  $\text{Li}_{3.75}\text{Mn}_{4.5}\text{Co}_{0.75}\text{O}_{12}$  composition yields a capacity of  $150 \text{ mAh g}^{-1}$  at  $25 \text{ mA g}^{-1}$  (equivalent to  $C/6$ ) with no perceptible capacity loss, in sharp contrast to the pure Mn materials.

## 2. Experimental

The compounds were prepared by solid state and solution methods. In the former case,  $\text{Li}_2\text{CO}_3$  (Aldrich, >99%),  $\text{MnCO}_3$  (Aldrich, purity >99.9%) and  $\text{Co}(\text{CH}_3\text{CO}_2)_2 \cdot 4\text{H}_2\text{O}$  (Aldrich, >98%) were ground intimately together in a mortar and pestle for 20 min. In the latter case  $\text{Mn}(\text{CH}_3\text{CO}_2)_2 \cdot 4\text{H}_2\text{O}$  (Aldrich, >99%) and  $\text{CO}(\text{CH}_3\text{CO}_2)_2 \cdot 4\text{H}_2\text{O}$  (Aldrich, >98%) were dissolved in distilled water to which a solution of  $\text{Li}_2\text{CO}_3$  in water was added. The resulting mixture was subjected to rotary evaporation in order to remove excess water. The rest of the synthetic procedure was identical regardless of whether the constituents were dry mixed or combined in an aqueous solution. The mixture was heated from room temperature to  $250^\circ\text{C}$  at  $3^\circ\text{C min}^{-1}$  held at this temperature for 8–10 h and then cooled at  $3^\circ\text{C min}^{-1}$  to room temperature. Subsequently, the sample was heated to  $430^\circ\text{C}$ – $440^\circ\text{C}$  at  $2^\circ\text{C min}^{-1}$  and held at this temperature for 20 h followed by cooling to room temperature at  $1^\circ\text{C min}^{-1}$ . At this stage, the sample was reground and refired at  $430^\circ\text{C}$ – $440^\circ\text{C}$ , followed by cooling to room temperature at  $1^\circ\text{C min}^{-1}$ . In the case of  $\text{Li}_4\text{Mn}_5\text{O}_{12}$ , firing was carried out at the slightly lower temperature of  $300$ – $395^\circ\text{C}$ .

The surface area for several compositions including the pure manganese compound was determined using the BET method and in all cases the values fell within the range  $5$ – $15 \text{ m}^2 \text{ g}^{-1}$ .

Powder X-ray diffraction was carried out using a Stoe STADI/P diffractometer operating with a focusing geometry in transmission mode. An Fe source was used to avoid the fluorescence associated with Mn samples when irradiated using a Cu source. A small angle position sensor detector was used for data collection. More detailed structural analysis was carried out using neutron diffraction on the Polaris diffractometer at The Rutherford-Appleton Laboratory. Since lithium and cobalt are neutron absorbers, the data were corrected for absorption. The structures were refined by the Rietveld method using the program TF12LS based on the Cambridge Crystallographic Subroutine Library (CSSL) [16,17]. Neutron scattering lengths of  $-0.19$ ,  $-0.3703$ ,  $0.278$  and  $0.5803$  ( $\text{all } \times 10^{-12} \text{ cm}$ ) were assigned to Li, Mn, Co and O, respectively [18]. Combined X-ray/neutron refinement was carried out using FULLPROF.99 [19].

Chemical analysis for lithium was carried out by flame emission and for manganese and cobalt by atomic absorption spectroscopy. The average oxidation state of the transition

metal ions was determined by redox titration using ferrous ammonium sulphate/KMnO<sub>4</sub>.

Electrochemical studies were conducted by fabricating composite electrodes using active material, Super S carbon and Kynar Flex 2801 binder in the weight ratios 85:10:5. The mixture was prepared as a slurry in THF and spread onto aluminium foil using the Doctor Blade technique. After evaporation of the solvent and drying, electrodes were incorporated into 2325 coin cells using lithium metal as the second electrode and a 1m (1 molal) solution of LiPF<sub>6</sub> (Hashimoto) in propylene carbonate (Merck) as electrolyte. Galvanostatic measurements were made using a Biologic Macpile II instrument.

## 3. Results and discussion

### 3.1. Structure and composition

Powder X-ray diffraction patterns collected over a range of compositions within the solid solutions series  $\text{Li}_{4-x}\text{Mn}_{5-2x}\text{Co}_{3x}\text{O}_{12}$ ,  $0 \leq x \leq 1$  are presented in Fig. 1. In each case the data may be indexed on a single cubic spinel phase within space group  $Fd\bar{3}m$ , confirming that a continuous range of solid solutions exist between the two end-members,  $\text{Li}_4\text{Mn}_5\text{O}_{12}$  and  $\text{LiMnCoO}_4$ . The lattice parameter decreases linearly with replacement of Li/Mn by Co from  $8.1350(6) \text{ \AA}$  at  $x = 0.0$  to  $8.0863(5) \text{ \AA}$  at  $x = 1$ .

Compositional analysis is presented in Table 1. There is good agreement between the observed compositions and those expected based on the stoichiometric ratios of the starting materials used in the synthesis of the compounds. In the case of  $x = 0$  it has, in the past, often proved difficult to prepare a compound with the stoichiometry  $\text{Li}_4\text{Mn}_5\text{O}_{12}$ , i.e. in which all the Mn is in the +4 oxidation state. Interestingly, Table 1 indicates that the solid state synthesis procedure employed in this paper does yield a material with a composition that is very close to the ideal stoichiometry. Table 1 also indicates that when prepared using the solution route, the  $x = 0$  composition is somewhat less oxidised and

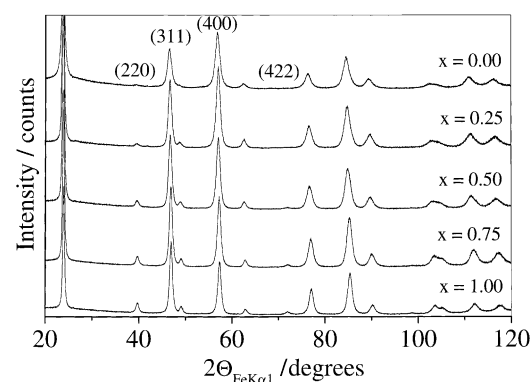


Fig. 1. Powder X-ray diffraction patterns for the solid solution series  $\text{Li}_{4-x}\text{Mn}_{5-2x}\text{Co}_{3x}\text{O}_{12}$  ( $0 \leq x \leq 1$ ).  $\text{Li}_4\text{Mn}_5\text{O}_{12}$  was synthesised by solid state reaction. All Co-doped samples were prepared via a solution route.

Table 1  
Chemical analysis results for  $\text{Li}_{4-x}\text{Mn}_{5-2x}\text{Co}_x\text{O}_{12}$  ( $0 \leq x \leq 1$ ) spinels

Nominal stoichiometry	Preparation route	Composition	Average transition metal oxidation state
$\text{Li}_{1.33}\text{Mn}_{1.67}\text{O}_4$ ( $x = 0.00$ )	Solution preparation	$\text{Li}_{1.390}\text{Mn}_{1.686}\text{O}_4$	3.920+
$\text{Li}_{1.33}\text{Mn}_{1.67}\text{O}_4$ ( $x = 0.00$ )	Solid state	$\text{Li}_{1.375}\text{Mn}_{1.661}\text{O}_4$	3.988+
$\text{Li}_{1.25}\text{Mn}_{1.5}\text{Co}_{0.25}\text{O}_4$ ( $x = 0.25$ )	Solution preparation	$\text{Li}_{1.292}\text{Mn}_{1.499}\text{Co}_{0.264}\text{O}_4$	3.805+
$\text{Li}_{1.25}\text{Mn}_{1.5}\text{Co}_{0.25}\text{O}_4$ ( $x = 0.25$ )	Solid state	$\text{Li}_{1.304}\text{Mn}_{1.495}\text{Co}_{0.266}\text{O}_4$	3.803+
$\text{Li}_{1.167}\text{Mn}_{1.333}\text{Co}_{0.5}\text{O}_4$ ( $x = 0.50$ )	Solution preparation	$\text{Li}_{1.190}\text{Mn}_{1.313}\text{Co}_{0.534}\text{O}_4$	3.685+
$\text{Li}_{1.167}\text{Mn}_{1.333}\text{Co}_{0.5}\text{O}_4$ ( $x = 0.50$ )	Solid state	$\text{Li}_{1.202}\text{Mn}_{1.314}\text{Co}_{0.540}\text{O}_4$	3.666+
$\text{Li}_{1.0833}\text{Mn}_{1.1667}\text{Co}_{0.75}\text{O}_4$ ( $x = 0.75$ )	Solution preparation	$\text{Li}_{1.080}\text{Mn}_{1.199}\text{Co}_{0.758}\text{O}_4$	3.535+
$\text{LiMnCoO}_4$ ( $x = 1.00$ )	Solution preparation	$\text{Li}_{0.996}\text{Mn}_{0.961}\text{Co}_{1.061}\text{O}_4$	3.463+

this is confirmed by X-ray and neutron diffraction data which indicates that the material prepared in solution exhibits a slightly larger cubic lattice parameter. For the Co-doped materials, X-ray, neutron diffraction and compositional analysis indicate that there is little difference between compounds prepared by the solution or the solid state route.

Detailed examination of Fig. 1 reveals that the intensities of the 220 and the 422 peaks relative to the other reflections, increase with increasing Co content which is indicative of an increase in the scattering from the tetrahedral 8a sites. To investigate this in more detail, neutron diffraction measurements were carried out on several compositions. Space does not permit a detailed presentation of the structural studies, this will be described elsewhere, however the salient features will be summarised here. The structure of the solid solution is based on that of the end-member  $\text{Li}_4\text{Mn}_5\text{O}_{12}$  ( $\text{Li}[\text{Li}_{1/3}\text{-Mn}_{5/3}]\text{O}_4$ ) [20]. The oxide ions adopts a cubic close packed arrangement and occupy the 32e positions of space group  $Fd\bar{3}m$ . Mn and Li occupy together half of the octahedral sites, designated 16d; this involves Li occupying 1/6 and Mn occupying 5/6 of the 16d sites. The remaining Li fully occupies 1/8 of the tetrahedral sites designated 8a. An interesting evolution of the structure occurs on raising the Co content which does not simply involve the replacement of Li and Mn on the 16d sites by Co. As  $x$  increases there is increasing occupancy of the tetrahedral, 8a, sites by Co and the corresponding displacement of lithium from the 8a to the 16d sites occurs such that the total occupancy of the 8a and 16d sites each remains close to unity. For  $x > 0.5$  the Li and Co ions on the 8a tetrahedral sites are displaced from the ideal 8a position, 0.125, 0.125, 0.125 to ( $x, x, x$ ) designated 32e. For  $x = 0.75$  the coordinates of the tetrahedral site are (0.1108(8), 0.1108, 0.1108). At this composition, the occupancy of the displaced tetrahedral sites are  $\text{Li}_{0.79}\text{Co}_{0.21}$  and of the octahedral 16d sites are  $\text{Li}_{0.15}\text{Mn}_{0.58}\text{Co}_{0.27}$ . At the upper Co limit corresponding to  $\text{LiMnCoO}_4$ , the occupancy of the tetrahedral sites by Co is 25%. Analysis of the neutron diffraction data do not provide any strong evidence for occupancy of the 16c sites, if there is any such occupancy it must be small. The occupancy of the tetrahedral site by Co raises the issue of the cobalt oxidation state. Studies are underway to determine the cobalt and manganese oxidation states in the solid solution series.

### 3.2. Electrochemical performance

The discharge capacities as a function of cycle number for a range of Co-doped solid solutions is shown in Fig. 2. All samples were prepared by the solution route except for  $\text{Li}_4\text{Mn}_5\text{O}_{12}$ . There is an overall trend of decreasing initial capacity with increasing cobalt content. Capacity fade is particularly severe at low Co doping levels. The best capacity retention is obtained at intermediate cobalt contents with the fade becoming somewhat more severe at  $x = 1$ . The best performance is obtained at  $x = 0.25$  which exhibits a capacity of  $>150 \text{ mAh g}^{-1}$  with no perceptible fade at the rate of  $25 \text{ mA g}^{-1}$ . X-ray diffraction data collected after cycling gives some indication as to the origin of the capacity fade for the Mn-rich compositions (Fig. 3). In the case of  $\text{Li}_4\text{Mn}_5\text{O}_{12}$  there is clear evidence of structural degradation on cycling. The X-ray data is consistent with a material exhibiting the features of two spinel structures, one with a lattice parameter similar to the original low temperature spinel and another with a lattice parameter close to the high temperature stoichiometric spinel  $\text{LiMn}_2\text{O}_4$ . It is known that the highly oxidised  $\text{Li}_4\text{Mn}_5\text{O}_{12}$  is metastable and will transform to a composition closer to the higher temperature  $\text{LiMn}_2\text{O}_4$  except when maintained under highly oxidising conditions [14,21]. It appears that on cycling, oxygen may be lost from the surface inducing compositional and structural inhomogeneity in the material. The X-ray data for the

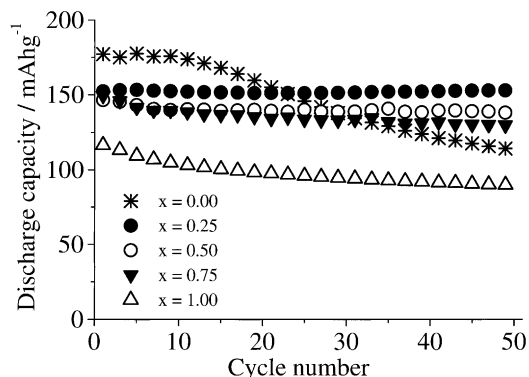


Fig. 2. Discharge capacity as a function of cycle number for  $\text{Li}_{4-x}\text{Mn}_{5-2x}\text{Co}_{3x}\text{O}_{12}$ . Rate =  $25 \text{ mA g}^{-1}$ , potential limits = 2.4–4.8 V.

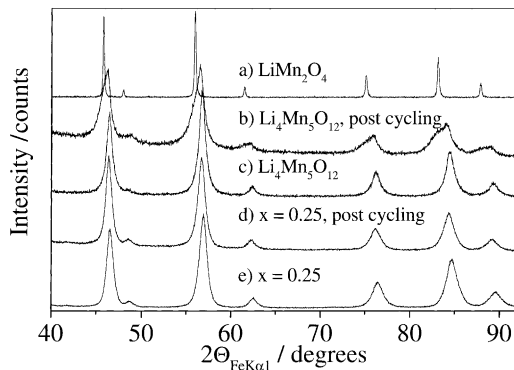


Fig. 3. Powder X-ray diffraction patterns for (a)  $\text{LiMn}_2\text{O}_4$  as-prepared; (b)  $\text{Li}_4\text{Mn}_5\text{O}_{12}$  after 50 cycles; (c)  $\text{Li}_4\text{Mn}_5\text{O}_{12}$  as-prepared; (d)  $x = 0.25$  after 50 cycles and (e)  $x = 0.25$  as-prepared. Note: X-ray patterns were collected after returning to 3.5 V.

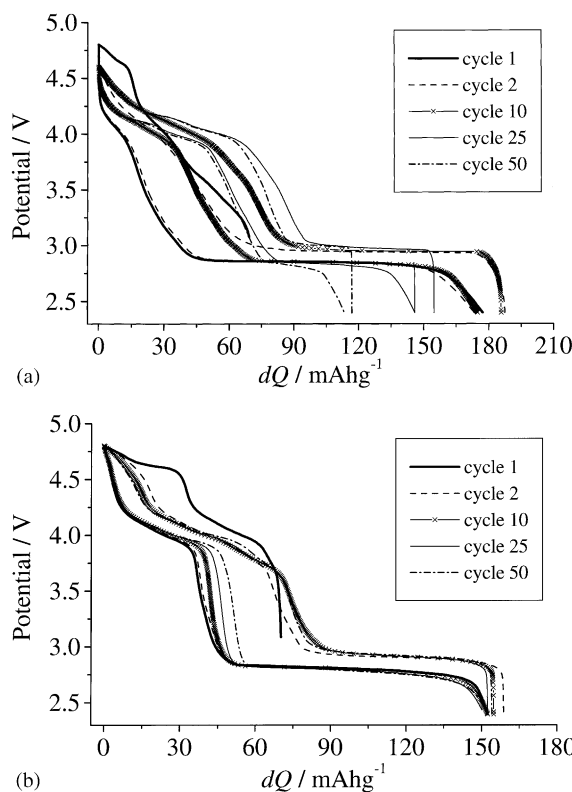


Fig. 4. Load curves for (a)  $\text{Li}_4\text{Mn}_5\text{O}_{12}$  and (b)  $\text{Li}_{3.75}\text{Mn}_{4.5}\text{Co}_{0.75}\text{O}_{12}$  ( $x = 0.25$ ).

Co-doped material (Fig. 3) does not show such degradation on cycling. It appears that the cobalt doping enhances the structural stability of the low temperature spinels compared with the pure manganese phase. Indeed it is known that the cobalt-rich end-member  $\text{LiMnCoO}_4$  can also be prepared at high temperatures in air which indicates increasing stability towards oxygen loss of the solid solutions as the cobalt content is increased.

Confirmation of the above structural results is seen in the load curves (Fig. 4). For  $\text{Li}_4\text{Mn}_5\text{O}_{12}$  prepared by solid state reaction there is little evidence of a 4 V plateau on the first charge/discharge cycle consistent with an oxidation state for manganese very close to +4. However, on cycling a significant double 4 V plateau develops and after some 25 cycles the load curve is reminiscent of high temperature spinel with an increasingly curtailed 3 V plateau and an ever greater capacity delivered at 4 V. In contrast, the load curves for  $x = 0.25$  exhibit some 4 V character on the first cycle, although most of the capacity is delivered at 3 V. This distribution and the load curves, in general for  $x = 0.25$ , are quite stable on cycling in contrast to the Mn-rich compositions.

## Acknowledgements

PGB is indebted to the EPSRC for financial support.

## References

- [1] A.D. Robertson, A.R. Armstrong, P.G. Bruce, Chem. Commun., submitted for publication.
- [2] M.M. Thackeray, W.I.F. David, W.I.F. David, P.G. Bruce, J.B. Goodenough, Mater. Res. Bull. 18 (1983) 461.
- [3] M.M. Thackeray, J. Electrochem. Soc. 142 (1995) 2558.
- [4] P.G. Bruce, J. Chem. Soc., Chem. Commun. 1997 (1997) 1817.
- [5] J.M. Tarascon, W.R. McKinnon, F. Coowar, T.N. Bowmer, G. Amatucci, D. Guyomard, J. Electrochem. Soc. 141 (1994) 1421.
- [6] Y. Gao, J.R. Dahn, J. Electrochem. Soc. 143 (1996) 100.
- [7] J.M. Tarascon, E. Wang, F.K. Shokoohi, W.R. McKinnon, S. Colson, J. Electrochem. Soc. 138 (1991) 2859.
- [8] L. Guohua, H. Ikuta, T. Uchida, M. Wakihara, J. Electrochem. Soc. 143 (1996) 178.
- [9] G. Pistoia, A. Antonini, R. Rosati, C. Bellitto, G.M. Ingo, Chem. Mater. 9 (1997) 1443.
- [10] A.D. Robertson, S.H. Lu, W.F. Averill, W.F. Howard Jr., J. Electrochem. Soc. 144 (1997) 3500.
- [11] A.D. Robertson, S.H. Lu, W.F. Averill, W.F. Howard Jr., J. Electrochem. Soc. 144 (1997) 3505.
- [12] P. Aitchison, B. Ammundsen, D.J. Jones, G. Burns, J. Rozière, J. Mater. Chem. 9 (1999) 3125.
- [13] M.M. Thackeray, A. De Kock, M.H. Russouw, D. Liles, R. Bittihn, D. Hoge, J. Electrochem. Soc. 139 (1992) 363.
- [14] M.N. Richard, E.W. Fuller, J.R. Dahn, Solid State Ionics 73 (1994) 81.
- [15] L. Sánchez, J.L. Tirado, J. Electrochem. Soc. 144 (1997) 1939.
- [16] J.C. Matthewman, P. Thompson, P.J. Brown, J. Appl. Crystallogr. 15 (1982) 167.
- [17] P.J. Brown, J.C. Matthewman, Rutherford-Appleton Laboratory Report, RAL-87-010 (1987).
- [18] V.F. Sears, Neutron News 3 (3) (1992) 26.
- [19] J. Rodriguez-Carvajal, FULLPROF.99 (Version 0.3), April 1999, LLB (unpublished).
- [20] T. Takada, E. Akiba, F. Izumi, B.C. Chakoumakos, J. Solid State Chem. 130 (1997) 74.
- [21] M.M. Thackeray, M.F. Mansuetto, C.S. Johnson, J. Solid State Chem. 125 (1996) 274.